Can a Dipole-Bound Electron Form a Pseudo-Atom? An Atoms-In-Molecules Study of the Hydrated Electron

ARTICLE *in* THE JOURNAL OF PHYSICAL CHEMISTRY A · NOVEMBER 2011

Impact Factor: 2.69 · DOI: 10.1021/jp207381t · Source: PubMed

3 AUTHORS, INCLUDING:

Qadir K Timerghazin
Marquette University
50 PUBLICATIONS **370** CITATIONS

SEE PROFILE

THE JOURNAL OF PHYSICAL CHEMISTRY A

ARTICLE

pubs.acs.org/JPCA

Can a Dipole-Bound Electron Form a Pseudo-Atom? An Atoms-In-Molecules Study of the Hydrated Electron

Qadir K. Timerghazin,*[,†] Inessa Rizvi,[‡] and Gilles H. Peslherbe*[,‡]

[†]Department of Chemistry, Marquette University, P.O. Box 1881, Milwaukee, Wisconsin, 53201

[‡]Centre for Research in Molecular Modeling and Department of Chemistry & Biochemistry, Concordia University, Montréal, QC, Canada H4B 1R6

Supporting Information

ABSTRACT: Non-nuclear local maxima, or attractors, of electron density are a rare but very interesting feature of the electron density distribution in molecules and solids. Recently, non-nuclear attractors (NNAs) and the corresponding pseudoatoms of electron density have been identified with the quantum theory of atoms in molecules for some anionic clusters formed by several polar solvent molecules and an excess electron bound in either a solvated-electron or dipole-bound fashion. This contribution reports a detailed study of the topology of the electron density for a series of dipole-bound water cluster anions, as calculated with Hartree−Fock, Møller−Plesset perturbation theory, and coupled-cluster methods together with basis sets augmented with extra diffuse basis functions to accommodate the excess electron. For dipole-bound clusters, electron densities obtained with insufficient inclusion of electron correlation effects and tight basis sets feature a well-pronounced pseudoatom due to the excess electron, which ultimately disappears when a higher level of electronic structure theory and a more diffuse basis set are used. On the other hand, for solvated-electron clusters, where the excess electron is surrounded by solvent molecules, the existence of NNAs does not seem to be an artifact of the method employed, but rather a genuine feature of the electron density distribution. Pseudoatoms of electron density thus appear to be an exclusive feature of confined environments and are unlikely to be found on the tip of a cluster dipole or on solid surfaces.

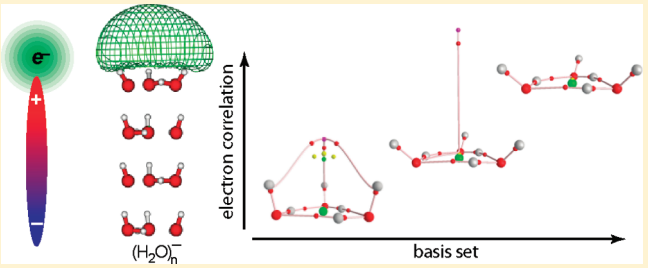

INTRODUCTION

The quantum theory of atoms in molecules[1] (QT AIM or in short AIM) enjoyed great success as a tool to analyze and rationalize chemical bonding in molecules, molecular assemblies, and solids.[2] Based on the analysis of the electron density $\rho(\mathbf{r})$, a physical observable that can be determined from electronic structure theory calculations or experimentally, AIM theory elegantly recovers some of the most fundamental concepts of chemistry. Traditional chemical notions, such as atoms being separate and transferable chemical entities or chemical bonds connecting atomic nuclei, are somewhat concealed in the wave function-based quantum-mechanical description of the molecular electronic structure. However, the topological analysis of $\rho(\mathbf{r})$ and its derivatives within the framework of AIM theory brings these concepts back to light. Whereas $\rho(\mathbf{r})$ itself only reflects the shape of the molecule, inspection of its first derivative, the gradient $\nabla\rho(\mathbf{r})$, allows the characterization of gradient paths and critical points (minima, maxima, saddle points) of the electron density that can be related to the classical concepts of chemical bonding. Local maxima, or attractors, of electron density usually correspond to atomic nuclei (nuclear critical points). Two nuclear critical points can be connected by a gradient path [atomic interaction line (AIL) or bond path], which corresponds to the line of maximum electron density between the two nuclei and is indicative of chemical bonding between the two atoms. Various numerical properties of the point of minimum electron density along a bond path (bond critical point, or BCP) characterize the nature of chemical bonding between two atoms. Zero-flux surfaces perpendicular to the bond paths at the BCP formally separate the atoms from each other in molecules (interatomic surfaces, or IASs). The AIM theory not only recovers the classical concepts of chemistry but also allows a quantitative description of chemical entities by providing useful metrics such as atomic charges, volumes, and energies, as well as the positions and properties of bond critical points, among others.

Remarkably, in some rare instances, electron density distributions can exhibit a maximum without an associated nucleus at this position, a feature usually referred to as a non-nuclear attractor (NNA). Just like for regular atoms, this maximum is separated

Special Issue: Richard F. W. Bader Festschrift

Received: August 2, 2011
Revised: September 1, 2011
Published: October 11, 2011

from nuclei by zero-flux interatomic surfaces and connected to some of them by atomic interaction lines or bond paths, thus giving rise to a *pseudoatom*. This topological entity has all the features of an atom in AIM theory, except for a nucleus at the point of maximum electron density. Although it is sometimes considered a fatal flaw of AIM theory, the very existence of pseudoatoms in systems such as metals or metal clusters[3] or *F*-centers in ionic crystals[4] can be intuitively understood and related to the chemical and physical properties of the system. In fact, experimental observations of NNAs in metals,[5] and very recently, organometallic compounds, have been reported.[6] However, it is also important to emphasize that, in some other cases, the observation of NNAs in computed electron densities turned out to be a mere artifact of an inappropriate basis set, as was reported for, e.g., Si−Si bonds.[1a,7]

Recently, NNAs were found in computed electron densities of cluster anions where the excess electron is surrounded by positive ends of dipolar molecules such as hydrogen fluoride,[8] acetonitrile,[9] and water.[10] There is currently a growing interest in these clusters, which are considered to be precursors of the bulk solvated electron,[11] and in their properties. The intuitive picture of the solvated electron as a distinct chemical species concurs well with the existence of a (pseudo)atom, showing once again how the results of AIM theory parallel chemical thinking.

Despite intense research in the area, the structure of water cluster anions, and thus the location of the excess (hydrated) electron in clusters and bulk water, remain controversial.[12] Even the traditional model of the hydrated electron residing in a solvent cavity[13] has recently been challenged.[12d,e] In addition to the cluster analogs of the solvated/hydrated electron, there is also another way to accommodate an excess electron without accepting it into the solvent's valence orbitals.[14] This diffuse dipole-bound electron (DBE) resides outside of the polar solvent cluster, or it may bind electrostatically even to a single solvent molecule dipole, if it is large enough.[14a] The nature of the interactions for the solvated and dipole-bound electrons are essentially the same, although the former is usually more tightly bound to the water cluster.

In our previous works,[8,9] we found that, unlike the solvated electron, which often gives rise to a NNA/pseudoatom of electron density, the dipole-bound electron is usually too diffuse to give rise to any specific signature in the topology of the electron density distribution. However, a clear signature of the excess electron can be identified by inspection of the topology of the Laplacian $\nabla^2\rho(\mathbf{r})$, the second derivative of the electron density, as a critical point characterizing the "dipole-bound charge concentration", i.e., a diffuse region outside the solvent molecule(s) where $\nabla^2\rho(\mathbf{r}) < 0$.[8,9]

Remarkably, Taylor et al.[10] recently reported a single case where, in a crown-like $(H_2O)_4^-$ cluster configuration (**cr4-1L**, Figure 1), the dipole-bound electron was found to give rise to a NNA/pseudoatom. None of the other dipole-bound isomers of water or other solvent cluster anions were reported to exhibit a NNA. Possibly, partial confinement from one side and a large enough dipole moment leading to tighter binding are responsible for the formation of the excess-electron pseudoatom in this case. One can imagine that keeping the same excess-electron binding motif, but increasing the dipole moment, would make it possible for this pseudoatom to localize on the tip of a "needle" (dipole). In this contribution, we present a study of the topology of the electron density in dipole-bound water cluster anions, with the excess-electron binding motif based on a "crown" of three and four water molecules (**cr3-1L** and **cr4-1L**, respectively, cf. Figure 1). The addition of extra layers of water molecules underneath the first one (Figure 1) affords a sharp increase of the excess-electron binding energ, from hereon referred to as the vertical detachment energy (VDE), and thus a more compact distribution of the excess electron.

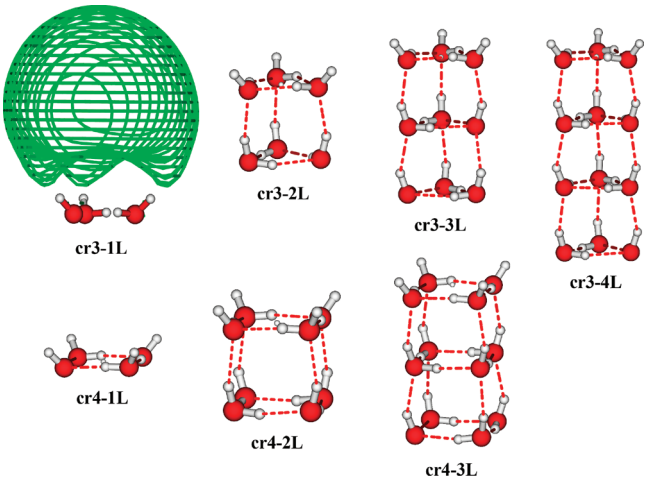

Figure 1. Structures of the dipole-bound water cluster anions investigated in this work. The typical shape of the diffuse singly occupied molecular orbital accommodating the excess electron is shown for the **cr3-1L** cluster.

Modeling of the excess-electron binding to polar solvent molecules in a dipole-bound or solvated-electron fashion is a challenging, although well understood, problem.[14b] First, it has been shown that the electrostatic interaction of the excess electron with the molecular or cluster dipole is only responsible for roughly half of the stabilization energy, with dispersion interactions accounting for the other half.[15] Thus, an extensive treatment of electron correlation, preferably with coupled-cluster theory with single and double excitations (CCSD) and perhaps even higher orders of excitation, is required. Interestingly, density-functional theory methods generally fail to properly describe systems with a dipole-bound electron and tend to significantly overestimate the excess-electron binding energy, possibly due to the self-interaction problem.[14b] The second important point is the diffusiveness and quality of the basis set used. The excess electron distribution is extremely diffuse in dipole-bound/solvated-electron systems, and thus, specially constructed diffuse basis sets are required, with extra diffuse basis functions often centered not on a particular atomic nucleus but rather on a floating "ghost" center.[16] The excess-electron binding is also sensitive to the quality of the valence basis set, with Dunnung's correlation-consistent basis sets yielding much more realistic VDE values than the Pople-style basis sets.[16] However, increasing the size of the valence basis sets, i.e., going from a double- to triple-ζ basis set, hardly improves the results.[16] Topological analyses of the electron density distribution in dipole-bound water cluster anions reported so far[10] were based on electron densities obtained using second-order Møller−Plesset (MP2) perturbation theory[17] calculations with a standard Pople-style 6-31++G(2d,2p) basis set. Considering the delicate nature of excess-electron binding in dipole-bound anions, we investigate in this contribution how the degree of inclusion of electron correlation and the choice of basis set influence the topology of the (excess) electron distribution.

COMPUTATIONAL METHODS

All electronic structure theory calculations were performed with the GAUSSIAN09 program suite.[18] Two split-valence basis sets were used: Dunning's aug-cc-pVDZ[19] and the Pople-style[17] 6-31++G^{++}, with the polarization functions proposed by Petersson et al.[20] To further asses the effects of the valence basis set, Dunning's triple-ζ aug-cc-pVTZ[19] basis set was also used in selected calculations. Each of these basis sets was augmented by nine shared-exponent diffuse sp-shells generated in an even-tempered manner, starting with the average of the most diffuse s- and p-exponents of the respective basis sets of the oxygen atom and a progression factor of 3.2, resulting in outmost exponents of $\sim 2.1 \times 10^{-6}$ and $\sim 2.4 \times 10^{-6}$, respectively.[16] These diffuse basis functions were placed in the plane of the topmost oxygen atoms along the symmetry axis of the cluster. We will refer to the resulting basis set combinations as avdz+9s9p and 6-31++G^{++}+9s9p. Alternative locations of the "ghost" basis center, including the positions of the oxygen/hydrogen atoms, were also tested, as well as less diffuse basis sets. To produce less diffuse basis sets, the most diffuse sp-shells were removed one by one, giving a series of 8s8p, 7s7p, ..., 1s1p basis sets.

Geometry optimizations were performed with second-order Møller−Plesset (MP2) perturbation theory[17] using the avdz+9s9s and 6-31++G^{++}+9s9s basis sets, and electron densities were produced at the Hartree−Fock (HF), MP2, and coupled-cluster[21] with single and double excitations[22] (CCSD) levels. All cluster anion calculations were performed with spin-unrestricted methods, and the resulting wave functions were found to be virtually free of spin contamination. The electron density analysis was performed using the AIMPAC program package,[23] and molecular graphs were generated with the AIM2000[24] and AIMAll[25] programs.

Excess-Electron Binding in Water Cluster Anions. The model systems investigated in this work are dipole-bound water cluster anions with three and four water molecules and a "crown" excess-electron binding motif (Figure 1). We will refer to these clusters by the number of water molecules forming the crown and the number of layers (or stacked crowns) in the cluster, e.g., **cr3-2L** refers to a cluster with a three-water-molecule electron-binding site and an additional three-water-molecule layer underneath. Excess-electron binding energies in these and similar clusters have been extensively studied in the literature.[14b,26] Thus, we will only briefly discuss the dependence of the VDE on the computational methods employed in this work (Table 1).

The excess electron is bound in all clusters investigated in this work; i.e., some energy is required to remove it from the cluster. However, the VDE varies widely depending on the level of inclusion of electron correlation and the type and size of basis set (Table 1). MP2 significantly underestimates the VDE values compared to CCSD, especially for clusters with a weakly bound excess electron. For instance, the VDE of **cr3-1L** calculated with MP2/avdz+9s9p is less than half of the CCSD/avdz+9s9p value (2.0 vs 5.1 meV). For more tightly bound clusters, this difference is less pronounced. Addition of the perturbative triples correction to the coupled-cluster treatment, CCSD(T), further increases the VDE, but the effect is much less dramatic than when going from MP2 to CCSD. Thus, CCSD electron densities can be used as a reliable high-level reference to assess the accuracy of the MP2 densities, which can be obtained for larger clusters for which CCSD calculations are not computationally practical.

Table 1. Calculated VDEs (meV) of Dipole-Bound Water Cluster Anions[a]

	water molecule layers			
	1 layer (n = 1)	2 layers (n = 2)	3 layers (n = 3)	4 layers (n = 4)
Three Water "Crown" **cr3-*n*L**				
MP2/avdz+9s9p	2	281	584	
CCSD/avdz+9s9p	5	321		
CCSD(T)/avdz+9s9p	6	343		
MP2/6-31++G^{++}+9s9p	0.4	247	533	737
CCSD/6-31++G^{++}+9s9p	0.8	273		
Four Water "Crown" **cr4-*n*L**				
MP2/avdz+9s9p	15	408		
CCSD/avdz+9s9p	26			
CCSD(T)/avdz+9s9p	30			
MP2/6-31++G^{++}+9s9p	4	349	680	
CCSD/6-31++G^{++}+9s9p	7	378		
CCSD(T)/ 6-31++G^{++}+9s9p	8			

[a] Refer to Figure 1 for cluster structures. All geometries were optimized at the MP2 level.

As noted previously in the literature, Pople-style split-valence basis sets, such as the 6-31++G^{++} used here, lead to highly underestimated VDE values (Table 1), although for the larger clusters, its performance lags behind that of aug-cc-pVDZ less dramatically. In fact, it has been suggested that the use of Pople-style basis sets judiciously augmented with extra atom-centered diffuse functions is a viable option for large water cluster anions for which calculations with more reliable basis sets become impractical.[26b] The addition of extra diffuse basis functions is essential for properly describing the excess-electron binding. For instance, if the number of diffuse basis functions in the even-tempered progression used (see Computational Methods) is decreased to four and two sp-shells (with the most diffuse exponents $\sim 7 \times 10^{-4}$ and $\sim 7 \times 10^{-3}$, respectively), the excess electron becomes unbound (negative VDE) for the **cr3-1L** and **cr4-1L** clusters (Figure 1). Thus, oversaturated diffuse 9s9p basis sets were used to preclude any possible artificial confinement of the excess electron that could affect VDE values and/or the topological features of the electron density distribution.

Addition of the first extra layer of water molecules beneath the excess-electron binding "crown" motif increases the VDE by one (from <30 to ~300 meV for **cr3**-clusters) to two (from <10 to <400 meV for **cr4**-clusters) orders of magnitude (Table 1). The VDE increase upon addition of more water layers is roughly additive, with each layer increasing the VDE by 250−300 meV. Considering the limitations of the method (MP2) and the valence basis set (6-31++G^{++}) used for the larger clusters (this combination tends to underestimate the VDE for small clusters, compared to coupled-cluster calculations, Table 1), the actual VDE for clusters with three and more layers may very well approach or even exceed 1 eV, in agreement with estimates by Drude model calculations (1221 meV for **cr4-3L**).[26a] Because of this dramatic increase in the VDE, one can expect significant changes in the electron density distribution associated with the dipole-bound electron distribution as cluster size increases.

Topology of the Electron Density Distribution. The topological features of the hydrogen-bonded network of water molecules

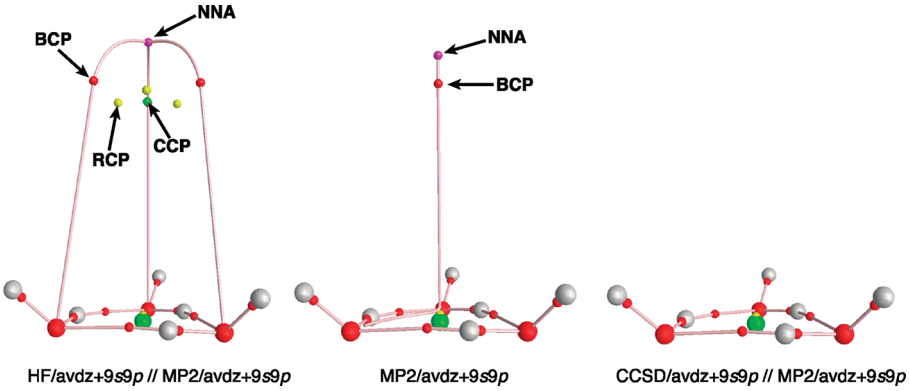

Figure 2. Molecular graphs of the **cr3-1L** water cluster anion for electron densities obtained with different levels of theory and the avdz+9s9p basis set. Important stationary points of the electron density are shown: non-nuclear attractors (NNAs, purple sphere), bond critical points (BCPs, small red sphere), cage critical points (CCPs, small green sphere), and ring critical points (RCPs, yellow spheres). Nuclei are connected to other nuclei or the NNA via atomic interaction lines (AILs)/bond paths shown in red. The "ghost" center of the diffuse basis functions is shown as a large green sphere.

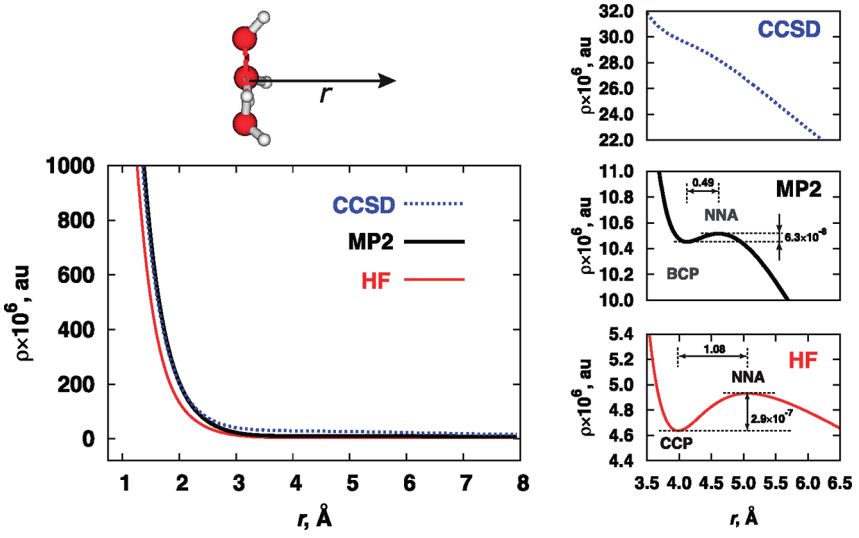

Figure 3. Electron density profiles along the symmetry axis of the **cr3-1L** water cluster anion calculated with different levels of theory and the avdz+9s9p basis set. The MP2/avdz+9s9p cluster geometry is used for all profiles. The plane of the three oxygen atoms defines the spatial reference (r = 0.0 Å). Enlarged portions of each profile in the NNA region are shown on the right-hand-side panels.

are well-known and largely unaffected by the addition of the dipole-bound electron. Thus, we concentrate on the topological features of the electron density arising solely from the presence of the excess electron.

Single-Layer Clusters. The molecular graphs for the **cr3-1L** cluster obtained from HF, MP2, and CCSD electron densities are shown in Figure 2. Clearly, the topological features of the electron density associated with the excess electron dramatically depend on the degree of the treatment of electron correlation. The HF molecular graph is similar to the molecular graph previously reported for the **cr4-1L** cluster:[10] the excess electron gives rise to a well-defined NNA and a corresponding pseudoatom of electron density. However, the AILs connect the NNA not to the hydrogen atoms of the water molecules, but rather to the oxygen atoms. Three ring critical points (RCPs) and one cage critical point (CCP) between the NNA-oxygen AILs are also observed, as required by the Poincaré−Hopf relationship, as discussed in detail in ref 10b. When some electron correlation is included at the MP2 level, the full-featured pseudoatom topology observed for the HF density starts to fold. Although a NNA is still observed, there is just a single AIL originating from it with a single BCP located nearby. This AIL follows the symmetry axis of the cluster until it almost reaches the RCP corresponding to the ring formed by the water molecules. Then, the AIL abruptly turns and heads to one of the oxygen atoms. Likely, the AIL is actually trifurcated at that point and connects to all three oxygen atoms, but we were only able to trace a single, nontrifurcated AIL. At the CCSD level, the topological features due to the excess electron disappear altogether and the only CPs and AILs observed are related to the intramolecular covalent bonding and the intermolecular hydrogen bonding of the water molecules.

The evolution of the maximum of electron density due to the presence of the excess electron can be clearly observed from electron density profiles along the cluster symmetry axis (Figure 3). Whereas on the larger scale (Figure 3a) the electron density seems to just rapidly decay as one moves away from the cluster, a more detailed inspection of the long tail (Figure 3b) shows that, for HF and MP2, the electron density first reaches a

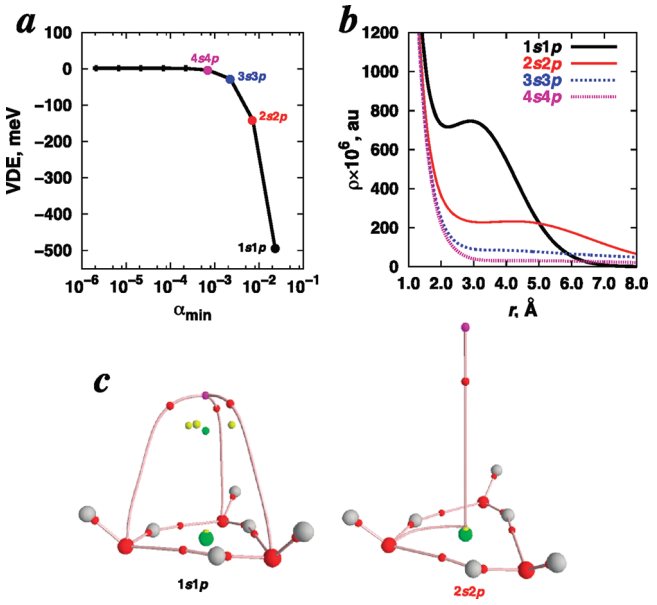

Figure 4. Properties of the electron density of the **cr3-1L** water cluster anion calculated at the MP2 level with the aug-cc-pVDZ basis set for different sizes of the additional diffuse basis set: (a) VDE; (b) electron density profile along the cluster symmetry axis (as in Figure 3); (c) molecular graphs.

minimum and then slightly increases, passing through a maximum (NNA), before decaying again. In the HF profile, the minimum corresponds to a CCP, whereas it is a BCP in the MP2 density.

The maximum and minimum in the HF density profile are separated by more than 1 Å, whereas in the MP2 profile they are much closer (∼0.5 Å). Also, the difference in the electron density between the maximum and minimum is an order of magnitude smaller at the MP2 level ($\Delta\rho = 6 \times 10^{-8}$ au vs 3×10^{-7} au for HF, Figure 3b). Thus, with the inclusion of electron correlation, and therefore higher VDE values, the excess electron distribution becomes flatter and the NNA less pronounced. Though the CCSD density is 2−3 times higher in the same region, the density profile shows only a decrease of electron density, with a slight shoulder where the minimum is observed in the HF and MP2 profiles (Figure 3b). We note that the profile of the CCSD density obtained for the **cr3-1L** cluster using the fully CCSD-optimized geometry is very similar to that obtained for the MP2 geometry, exhibiting no minimum and one maximum (Figure S1, Supporting Information). Thus, as the electron becomes more strongly bound to the water cluster due to electron correlation, the NNA and other topological features related to it (AILs and bond, ring and cage CPs) disappear. On the other hand, the HF density exhibits a distinct NNA, whereas the method predicts an almost unbound excess electron, with a VDE of ∼1.2 meV.

Figure 4 demonstrates the effect of the diffusiveness of the basis set on the calculated VDE and the density profile at the MP2 level with the aug-cc-pVDZ valence basis set for the **cr3-1L** cluster. As one starts with the full 9s9p extra diffuse basis set and removes outmost sp-shells one by one, the VDE changes very little down to five sp-shells, but it quickly becomes negative when additional diffuse shells are stripped off. At the MP2/avdz+1s1p level, the negative VDE of the excess electron is as large as ∼0.5 eV in magnitude (Figure 4a). As the diffusiveness of the basis set decreases, the excess electron localizes in the immediate vicinity of the water cluster (Figure 4b). At the same time, the maximum and minimum in the density profile become more pronounced. The topology of the electron density distribution with two and more diffuse sp-shells is essentially the same, with a single AIL connecting the NNA to the water cluster (Figure 4c). On the other hand, with MP2/avdz+1s1p, which predicts a highly unstable excess electron confined by a tight basis set, one can observe a well-defined NNA connected by AILs to the three oxygen atoms. This topology is essentially identical to that observed for the HF density (Figure 2). If the MP2/avdz+1s1p geometry is used instead of the MP2/avdz+9s9p one, the topology slightly changes, with the AILs connecting the NNA to the hydrogen atoms, and not to the oxygen atoms (Figure S2, Supporting Information), giving essentially the same topology as that reported in ref 10 for the larger **cr4-1L** cluster.

The topology of the electron density due to the excess electron does not seem to depend on the quality of the valence basis set. Although the 6-31++G^{++}+9s9p basis set yields much lower VDEs, the density profiles calculated with this basis set (Figure S3, Supporting Information) are quantitatively similar to those calculated with the higher-quality aug-cc-pVDZ basis set (Figure 3). We note that the profiles of the CCSD density obtained with double- and triple-ζ valence basis sets (avdz+9s9p and avtz+9s9p) for the **cr3-1L** cluster are essentially the same, exhibiting no minimum/maximum pattern (Figure S1, Supporting Information), confirming that the double-ζ aug-cc-pVDZ valence basis set is adequate and one does not need to employ a larger valence basis set for the purpose at hand.

For the larger four-water cluster **cr4-1L**, the evolution of the NNA with the increasing level of treatment of electron correlation is similar to that for the **cr3-1L** cluster. Both HF and MP2 densities obtained with the avdz+9s9p basis set demonstrate a minimum and a maximum of electron density along the symmetry axis (Figure 5), whereas these features disappear in the CCSD profile, where only a shoulder is observed. However, unlike for the three-water cluster, the topology of the MP2 electron density is similar to its HF counterpart, with the NNA connected by four AILs to the oxygen atoms, with a corresponding set of three BCPs, three RCPs, and a CCP. In the MP2 case, these critical points lie much closer to each other, suggesting a much smoother electron density distribution, and the instability of the topology with respect to changes in geometry, consistent with the results of ref 10. However, in this work, the AILs connect the NNA to the oxygen atoms, not to the hydrogen atoms as was reported in ref 10, where a much less diffuse basis set was employed.

The CCSD density obtained for the **cr4-1L** cluster with a high-quality avdz+9s9p basis set does not exhibit a NNA, very much like in the case of the **cr3-1L** cluster. However, with CCSD/6-31++G^{++}+9s9p, which predicts VDE values more than 6 times smaller (0.8 vs 5.1 meV, Table 1), the electron density has a topology similar to that of the HF and MP2 densities, with a NNA present (Figure S4, Supporting Information). In fact, this is the only case that a NNA is observed in a CCSD density in this work.

Multilayer Clusters. Addition of one to three extra water layers beneath the first layer of the **cr3** cluster leads to a dramatic increase of the VDE (Table 1). However, the maximum of electron density due to the excess electron disappears and only a shoulder can be observed in the MP2 densities obtained with both valence basis sets used (Figure 6). This shoulder becomes

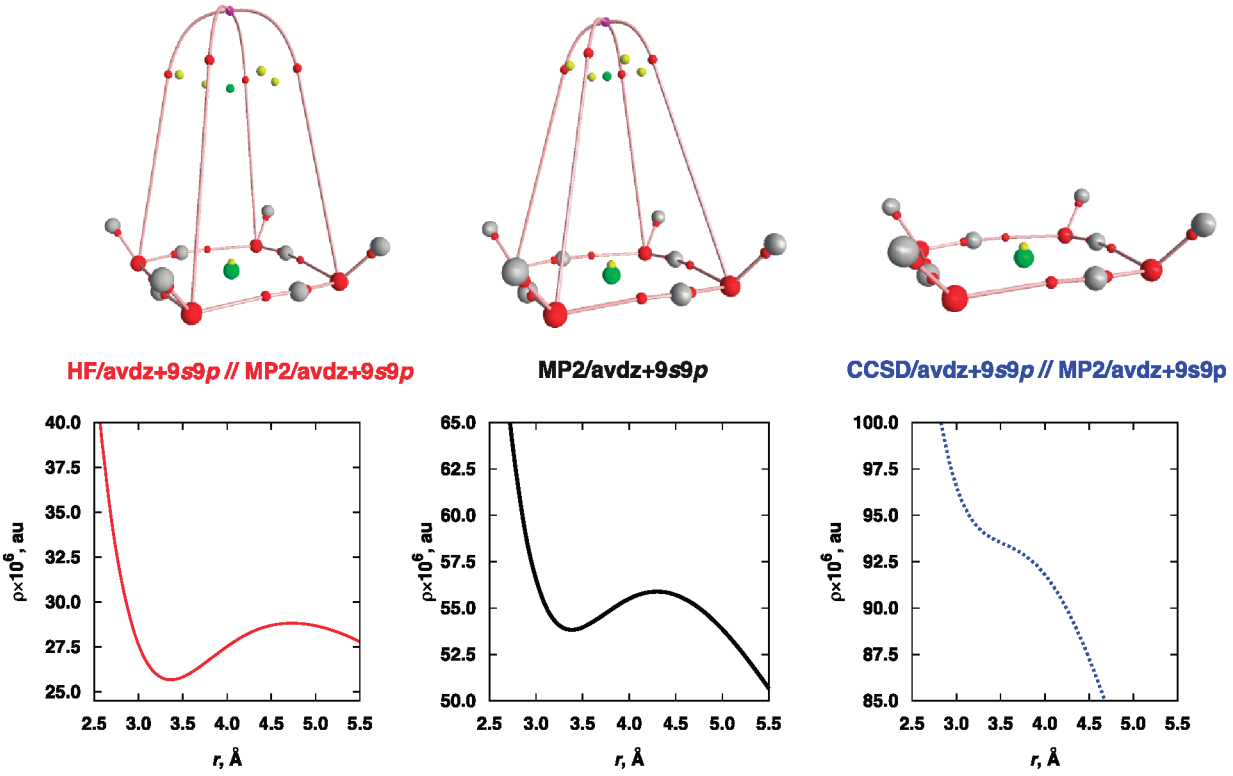

Figure 5. Molecular graphs (top panels) and electron density profiles along the symmetry axis in the NNA region (bottom panels) of the **cr4-1L** water cluster anion for electron densities obtained with different levels of theory and the avdz+9s9p basis set. The MP2/avdz+9s9p cluster geometry is used throughout.

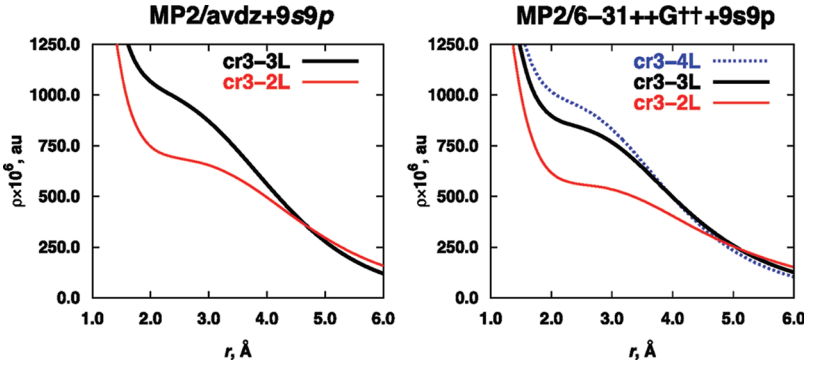

Figure 6. Electron density profiles for the **cr3-2L**, **cr3-3L**, and **cr3-4L** water cluster anions along the cluster symmetry axis calculated with MP2/avdz +9s9p and MP2/6-31++$G^{††}$+9s9p.

less and less prominent as the electron binding energy increases upon addition of water layers, despite the fact that the excess electron distribution becomes increasingly more compact.

For clusters with the four-water excess-electron binding motif, addition of the second water layer does not make the NNA disappear at the MP2 level (Figures 7 and S5, Supporting Information). Again, HF densities exhibit a pronounced NNA whereas the NNA disappears at the CCSD level. With the addition of a third layer, i.e., for the **cr4-3L** cluster, the HF/6-31++$G^{††}$+9s9p profile still has a prominent maximum, whereas the MP2/6-31++$G^{††}$+9s9p profile appears to exhibit an extended shoulder (Figure S6a, Supporting Information), which actually contains a faint local minimum and maximum. These extrema are separated by <0.2 Å, with a difference of electron density of only $\sim 5 \times 10^{-8}$ au (Figure S6b, Supporting Information). These features would most likely disappear with a better valence basis set at the MP2 level.

GENERAL DISCUSSION

In the analysis of the profiles and topologies of the electron density for the dipole-bound water cluster anions investigated here, a clear trend seems to emerge: as model chemistries that include more dynamic electron correlation and/or better valence and diffuse basis sets are used, the NNA of electron density and corresponding pseudoatom due to the excess electron becomes less and less pronounced and ultimately disappears. HF densities always have a well-defined minimum-maximum density pattern

and a well-developed pseudoatom topology due to the excess electron. MP2 electron density distributions in the region of the NNA tend to be flatter, with the minima and maxima getting closer together, and with smaller differences in the absolute values of the electron density. At the CCSD level, the NNA disappears entirely if an adequate valence basis set is employed (Figures 2, 5, 7, and S1 and S3, Supporting Information).

Along similar lines, "tighter" diffuse basis sets lead to significantly underestimated or even negative VDE values, and a pronounced NNA/pseudoatom, which tends to disappear when additional diffuse basis functions with smaller exponents are added (Figure 4). Pople-style basis sets, which produce results that significantly underestimate the excess-electron binding, may lead to a NNA that is not observed with the better aug-cc-pVDZ basis set, which incidentally also yields much more realistic VDE values (Figures 5 vs S4, Supporting Information). For densities obtained with methods that include electron correlation, the NNA disappears for multilayer clusters, even though it may be observed with the same method for the single-layer cluster (Figure 6). Thus, the stronger the excess-electron binding, the stronger it clings to the water molecules, and as one moves away from the host cluster, the electron density just decays without forming a NNA/pseudoatom of electron density.

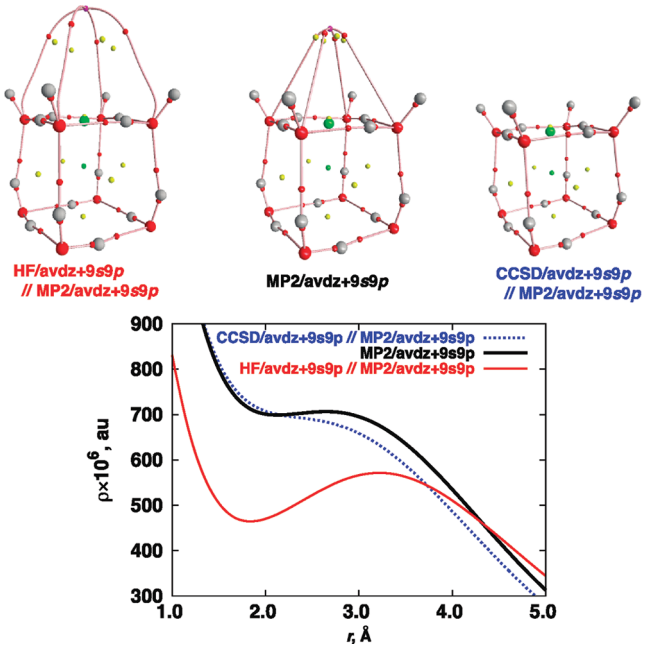

Figure 7. Molecular graphs (top panels) and electron density profiles along the symmetry axis in the NNA region (bottom panel) of the **cr4-2L** water cluster anion for electron densities obtained with different levels of theory and the avdz+9s9p basis set. The MP2/avdz+9s9p cluster geometry is used throughout.

With this understanding, it is possible to make the excess electron form a NNA/pseudoatom of electron density by reducing the degree of inclusion of electron correlation and/or the diffusiveness of the basis set. For example, the **cr3-4L** cluster has the highest VDE calculated in this work (>0.7 eV with MP2/6-31++G^{++}+9s9p, Table 1), and it does not exhibit a NNA in the MP2 electron density (Figure 8). However, if one uses the HF method, which does not include electron correlation at all, and one reduces the diffuse basis set to a single sp-shell, a prominent artificial maximum of electron density is readily observed (Figure 8).

Interestingly, **cr4-*n*L** clusters tend to exhibit a more pronounced NNA for more combinations of method and basis set than **cr3-*n*L** clusters, which bind the excess electron less strongly. This may be related to a better encompassing of the excess electron by the four-water clusters. Nevertheless, for any cluster considered in this work, the excess electron NNA/pseudoatom ultimately disappears when an improved model chemistry is employed.

Therefore, it appears that the NNA and the corresponding pseudoatom of electron density in dipole-bound water cluster anions is a mere artifact of inadequate computational methods employed to obtain the electron density. One may thus wonder whether the pseudoatoms observed in the calculated electron densities for water clusters with a "solvated" excess electron surrounded by water molecules[10] is also just an artifact of the computational method employed. Unlike the NNA for the excess electron dipole-bound to a cluster of polar molecules, NNAs and the corresponding pseudoatoms were observed previously for the (solvated-electron) hydrogen fluoride trimer $(HF)_3^-$ and acetonitrile dimer $(CH_3CN)_2^-$ cluster anions in electron densities calculated at the CCSD level with high-quality basis sets with extra diffuse basis functions.[8,9] Thus, pseudoatoms due to the solvated electron in water clusters reported previously[8,9] may also be a genuine feature of the electron density for these systems. Indeed, MP2 calculations using basis sets augmented with extra diffuse functions show a well-defined pseudoatom topology for

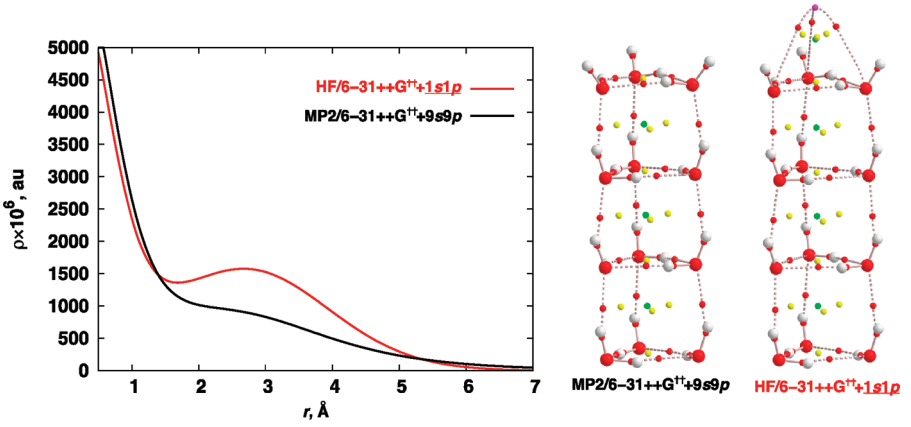

Figure 8. Electron density profiles along the cluster symmetry axis (left) and corresponding molecular graphs (right) of the **cr3-4L** water cluster anions calculated with MP2/6-31++G^{++}+9s9p and HF/6-31++G^{++}+1s1p. The MP2/6-31++G^{++}+9s9p geometry is used throughout.

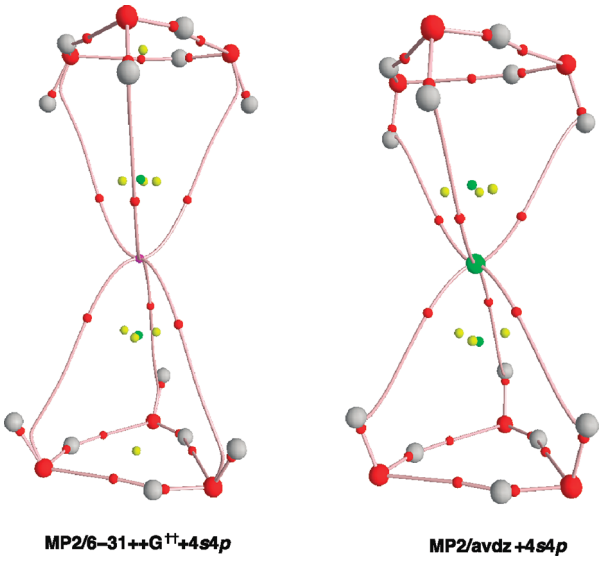

Figure 9. Molecular graphs of the solvated-electron water hexamer cluster anion calculated with MP2/6-31++G††+4s4p and MP2/avdz+4s4p.

the solvated-electron water hexamer anion (Figure 9). This cluster has an excess-electron binding motif similar to that in the **cr3-*n*L** clusters considered in this work (Figure 1), but with the excess electron suspended between two crown-like water trimers. Interestingly, although the existence of the NNA does not depend on the valence basis set used, some topological features of the electron density do. Specifically, the AILs connecting the NNA to water molecules terminate at either the oxygen or hydrogen atoms. This is indicative of a very floppy distribution of the excess electron density in the solvent cavity, with topological features strongly dependent even on small variations in the basis set. A similar unstable topology due to the very flat distribution of the (excess) electron density was reported for pseudoatoms corresponding to *F*-centers in ionic crystals.[4a] In that case, the NNA was even reported to split into a set of a few interconnected NNAs for some basis sets.[4a] This leads us to question the very concept of well-defined "bonds"[10a] between the solvated electron and specific atoms of the molecules surrounding the excess electron.

The question remains as to whether a NNA may exist for an electron loosely attached to the surface of a cluster or a solid and not surrounded by molecules in a solvated-electron fashion. Results of this work suggest that it is unlikely. However, we note that the HF method, which essentially describes the excess electron bound to the cluster exclusively by electrostatic forces with no dispersion interaction contribution, tends to yield electron densities with NNAs. Thus, in systems where the dispersion interactions play a minor role in the binding of the excess electron, it is plausible that a pseudoatom of electron density indeed exists. But again, as dispersion interactions seem to play a critical role for almost all systems with a dipole-bound electron,[14b] it is very unlikely that an excess electron gives rise to a NNA/pseudoatom in any of these dipole-bound systems.

The fact that the dipole-bound electron does not give rise to any topological markers in the electron density does not mean that the QTAIM-based analyses are not useful for the characterization of the dipole-bound electron distribution. We previously have shown[8,9] that the excess electron in dipole-bound or solvated-electron systems always gives rise to a very characteristic region of space with a negative Laplacian of the electron density. The topology of the Laplacian and the properties of its critical points can thus serve as useful metrics to quantitatively describe the excess electron distribution.[8,9]

CONCLUSIONS

In this article, we report a careful investigation of the occurrence of pseudoatoms of electron density for dipole-bound water cluster anions. For electron densities obtained with model chemistries that underestimate the excess-electron binding due to an insufficient degree of dynamic electron correlation and/or an inadequate basis set, NNAs and the corresponding pseudoatoms are indeed observed. However, the dipole-bound electron giving rise to a pseudoatom of electron density turns out to be a mere artifact of an inadequate method, as this feature consistently disappears with improved computational methods that adequately describe the excess-electron binding to the cluster. In fact, NNAs and the corresponding pseudoatoms appear to be a feature of electron distributions only in confined environments. Although genuine pseudoatoms are indeed observed theoretically and experimentally in some systems, this work once again demonstrates that NNAs in calculated electron densities may often be an artificial result of the use of an inappropriate method and/or basis set. Properties of the critical points of the Laplacian of the electron density, however, could be a more robust metric to characterize the excess electron distribution in dipole-bound anions.

ASSOCIATED CONTENT

Supporting Information. Electron density profiles and molecular structures (Figures S1−S6). Cartesian coordinates and energies for all calculated cluster structures. This material is available free of charge via the Internet at http://pubs.acs.org.

AUTHOR INFORMATION

Corresponding Author

*E-mail: Q.K.T., qadir.timerghazin@mu.edu; G.H.P., gilles.peslherbe@concordia.ca.

ACKNOWLEDGMENT

The calculations were performed at the Centre for Research in Molecular Modeling (CERMM), which was established with the financial support of Concordia University, the Ministère de l'Éducation du Québec (MEQ), and the Canada Foundation for Innovation (CFI), and on the high-performance computing cluster *Père* at Marquette University funded by National Science Foundation (NSF) awards (OCI-0923037 and CBET-0521602). Q.K.T. acknowledges financial support from Marquette University while completing this work. G.H.P. holds a Concordia University Research Chair and acknowledges the Natural Sciences and Engineering Research Council (NSERC) of Canada for partial funding of this work. A preliminary account of this work was first presented by IR at the 87th Canadian Society for Chemistry Conference, in London, Ontario, in 2004.

REFERENCES

(1) (a) Bader, R. F. W. *Atoms in Molecules: A Quantum Theory*; Oxford University Press: Oxford, U.K., 1990. (b) Popelier, P. L. A. *Atoms in Molecules: An Introduction*; Pearson Education: London, 2000.

(2) Matta, C. F.; Boyd, R. J. *The Quantum Theory of Atoms in Molecules: From Solid State to DNA and Drug Design*; Wiley-VCH: New York, 2007.
(3) (a) Bersuker, G. I.; Peng, C. Y.; Boggs, J. E. *J. Phys. Chem.* **1993**, *97*, 9323. (b) Luaña, V.; Costales, A.; Mori-Sanchez, P.; Blanco, M. A.; Pendas, A. M. *Acta Crystallogr.* **2004**, *A60*, 434. (c) Luaña, V.; Mori-Sánchez, P.; Costales, A.; Blanco, M. A.; Pendás, A. M. *J. Chem. Phys.* **2003**, *119*, 6341. (d) Pendás, A. M.; Blanco, M. A.; Costales, A.; Mori-Sánchez, P.; Luaña, V. *Phys. Rev. Lett.* **1999**, *83*, 1930. (e) Friis, J.; Madsen, G. K. H.; Larsen, F. K.; Jiang, B.; Marthinsen, K.; Holmestad, R. *J. Chem. Phys.* **2003**, *119*, 11359. (f) Madsen, G. K. H.; Blaha, P.; Schwarz, K. *J. Chem. Phys.* **2002**, *117*, 8030.
(4) (a) Bader, R. F. W.; Platts, J. A. *J. Chem. Phys.* **1997**, *107*, 8545. (b) Madsen, G. K. H.; Gatti, C.; Iversen, B. B.; Damjanovic, L.; Stucky, G. D.; Srdanov, V. I. *Phys. Rev. B* **1999**, *59*, 12359. (c) Madsen, G. K. H.; Iversen, B. B.; Blaha, P.; Schwarz, K. *Phys. Rev. B* **2001**, *64*, 195102.
(5) Iversen, B. B.; Larsen, F. K.; Souhassou, M.; Takata, M. *Acta Crystallogr.* **1995**, *B51*, 580.
(6) Platts, J. A.; Overgaard, J.; Jones, C.; Iversen, B. B.; Stasch, A. *J. Phys. Chem. A* **2011**, *115*, 194.
(7) Zhikol, O. A.; Oshkalo, A. F.; Shishkin, O. V.; Prezhdo, O. V. *Chem. Phys.* **2003**, *288*, 159.
(8) Timerghazin, Q. K.; Peslherbe, G. H. *J. Chem. Phys.* **2007**, *127*, 064108.
(9) Timerghazin, Q. K.; Peslherbe, G. H. *J. Phys. Chem. B* **2007**, *112*, 520.
(10) (a) Taylor, A.; Boyd, R. J. *Phys. Chem. Chem. Phys.* **2008**, *10*, 6814. (b) Taylor, A.; Matta, C. F.; Boyd, R. J. *J. Chem. Theory Comput.* **2007**, *3*, 1054.
(11) Ben-Amotz, D. *J. Phys. Chem. Lett.* **2011**, *2*, 1216.
(12) (a) Turi, L.; Sheu, W.-S.; Rossky, P. J. *Science* **2005**, *310*, 1769c. (b) Turi, L.; Sheu, W.-S.; Rossky, P. J. *Science* **2005**, *309*, 914. (c) Verlet, J. R. R.; Bragg, A. E.; Kammrath, A.; Cheshnovsky, O.; Neumark, D. M. *Science* **2005**, *310*, 1769b. (d) Larsen, R. E.; Glover, W. J.; Schwartz, B. J. *Science* **2010**, *329*, 65. (e) Larsen, R. E.; Glover, W. J.; Schwartz, B. J. *Science* **2011**, *331*, 1387. (f) Jacobson, L. D.; Herbert, J. M. *Science* **2011**, *331*, 1387. (g) Turi, L.; Madarász, Á. *Science* **2011**, *331*, 1387.
(13) (a) Hart, E. J.; Anbar, M. *The Hydrated Electron*; Wiley-Interscience: New York, 1970; 288 pp. (b) Kevan, L. *Acc. Chem. Res.* **1981**, *14*, 138.
(14) (a) Jordan, K. D.; Luken, W. *J. Chem. Phys.* **1976**, *64*, 2760. (b) Jordan, K. D.; Wang, F. *Annu. Rev. Phys. Chem.* **2003**, *54*, 367.
(15) (a) Gutowski, M.; Jordan, K. D.; Skurski, P. *J. Phys. Chem. A* **1998**, *102*, 2624. (b) Gutowski, M.; Skurski, P. *J. Phys. Chem. B* **1997**, *101*, 9143. (c) Gutowski, M.; Skurski, P. *J. Chem. Phys.* **1997**, *107*, 2968. (d) Gutowski, M.; Skurski, P.; Boldyrev, A. I.; Simons, J.; Jordan, K. D. *Phys. Rev. A* **1996**, *54*, 1906. (e) Gutowski, M.; Skurski, P.; Jordan, K. D.; Simons, J. *Int. J. Quantum Chem.* **1997**, *64*, 183.
(16) Skurski, P.; Gutowski, M.; Simons, J. *Int. J. Quantum Chem.* **2000**, *80*, 1024.
(17) Hehre, W. J.; Radom, L.; Schleyer, P. v. R.; Pople, J. A. *Ab Initio Molecular Orbital Theory*; John Wiley and Sons: New York, 1985.
(18) Frisch, M. J.; Trucks, G. W.; Schlegel, H. B.; Scuseria, G. E.; Robb, M. A.; Cheeseman, J. R.; Scalmani, G.; Barone, V.; Mennucci, B.; Petersson, G. A.; Nakatsuji, H.; Caricato, M.; Li, X.; Hratchian, H. P.; Izmaylov, A. F.; Bloino, J.; Zheng, G.; Sonnenberg, J. L.; Hada, M.; Ehara, M.; Toyota, K.; Fukuda, R.; Hasegawa, J.; Ishida, M.; Nakajima, T.; Honda, Y.; Kitao, O.; Nakai, H.; Vreven, T.; Montgomery, J. A., Jr.; Peralta, J. E.; Ogliaro, F.; Bearpark, M.; Heyd, J. J.; Brothers, E.; Kudin, K. N.; Staroverov, V. N.; Kobayashi, R.; Normand, J.; Raghavachari, K.; Rendell, A.; Burant, J. C.; Iyengar, S. S.; Tomasi, J.; Cossi, M.; Rega, N.; Millam, N. J.; Klene, M.; Knox, J. E.; Cross, J. B.; Bakken, V.; Adamo, C.; Jaramillo, J.; Gomperts, R.; Stratmann, R. E.; Yazyev, O.; Austin, A. J.; Cammi, R.; Pomelli, C.; Ochterski, J. W.; Martin, R. L.; Morokuma, K.; Zakrzewski, V. G.; Voth, G. A.; Salvador, P.; Dannenberg, J. J.; Dapprich, S.; Daniels, A. D.; Farkas, Ö.; Foresman, J. B.; Ortiz, J. V.; Cioslowski, J.; Fox, D. J. *Gaussian 09*, Revision B.01; Gaussian, Inc.: Wallingford, CT, 2009.
(19) Dunning, T. H., Jr. *J. Chem. Phys.* **1989**, *90*, 1007.
(20) (a) Petersson, G. A.; Al-Laham, M. A. *J. Chem. Phys.* **1991**, *94*, 6081. (b) Petersson, G. A.; Bennett, A.; Tensfeldt, T. G.; Al-Laham, M. A.; Shirley, W. A.; Mantzaris, J. *J. Chem. Phys.* **1988**, *89*, 2193.
(21) Cizek, J. *Adv. Chem. Phys.* **1969**, *14*, 35.
(22) Purvis, G. D., III; Bartlett, R. J. *J. Chem. Phys.* **1982**, *7V6*, 1910.
(23) AIMPAC, Available from Professor R. F. W. Bader, McMaster University, Hamilton, ON L8S 4M1, Canada, and from AIMPAC website (http://www.chemistry.mcmaster.ca/aimpac/).
(24) Biegler-König, F.; Schönbohm, J.; Bayles, D. *J. Comput. Chem.* **2001**, *22*, 545.
(25) Keith, T. A. *AIMAll* (Version 11.06.19); TK Gristmill Software (aim.tkgristmill.com): Overland Park, KS, U.S.A., 2011.
(26) (a) Sommerfeld, T.; Jordan, K. D. *J. Am. Chem. Soc.* **2006**, *128*, 5828. (b) Herbert, J. M.; Head-Gordon, M. *J. Phys. Chem. A* **2005**, *109*, 5217.